

Dimethyl Sulfide Formation from Adsorbed Methanethiol: Surface Trapping of UV-Generated Reaction Intermediates

Nicholas Camillone III,^{*,†,‡,§} Kaveh Adib,^{†,||} Khalid A. Khan,[†] Dan Mocuta,[†] and Richard M. Osgood, Jr.^{†,‡}

Columbia Radiation Laboratory and Materials Science Program, Department of Applied Physics and Applied Mathematics, Columbia University, New York, New York 10027, and Brookhaven National Laboratory, Upton, New York 11973

Received: June 5, 2002; In Final Form: September 26, 2002

We present studies of the photoinduced surface chemistry of methanethiol adsorbed on GaAs(110). UV irradiation of these molecules, which are intact at ~ 90 K, induces scission of the S–H bond, leaving the CH_3S fragment trapped at the surface. The measured cross section at 193 nm for this photoinduced process is $\sim 3.6 \times 10^{-20} \text{ cm}^2$. Postirradiation heating of the surface-bound products of the methanethiol photoreaction results in the evolution of dimethyl sulfide with the same desorption kinetics as observed for the strictly thermal production of dimethyl sulfide from dissociatively adsorbed methyl disulfide. Thus, UV irradiation of $\text{CH}_3\text{SH}/\text{GaAs}(110)$ followed by thermal activation of the surface-trapped intermediates is shown to provide a new route to partial desulfurization of CH_3SH .

1. Introduction

Organosulfur compounds in general, and normal alkane thiols $[\text{CH}_3(\text{CH}_2)_{n-1}\text{SH}]$ in particular, are of interest for a variety of applications using functional, ordered monolayers on solid surfaces. These applications range from ultrathin electron-beam lithographic resists to model surface layers for the study of interfacial electron transfer to functionalized monolayers in advanced electronic sensors. Questions concerning the molecular-scale properties of these layers are central to their engineering utility.

As a result, there has been an expansion of interest in the investigation of the fundamental chemistry of these molecular layers. For example, the molecular structure, chemistry, and growth of thiol monolayers with $n > 4$ adsorbed on gold surfaces have been examined extensively using a wide variety of surface characterization techniques including infrared spectroscopy, glancing incidence X-ray diffraction, helium diffraction, X-ray photoelectron spectroscopy, and scanning probe microscopy.¹ These data have shown the binding energy and orientation of the adsorbed molecules, as well as factors leading to their molecular ordering. More recently, other studies have examined the chemistry of thiols on Au in the presence of surface excitation such as surface X-ray and electron bombardment.

Despite the widespread interest in adsorbed thiol chemistry and the fact that many applications envisioned for thiols involve semiconductor surfaces, remarkably few studies of thiol chemistry on semiconductor surfaces have been done. In particular, at present, comparatively little information is available concern-

ing the chemistry and physical interactions of thiols and related compounds with semiconductor surfaces.^{2,3}

In this paper, we report on the UV-initiated chemistry of thiol molecules adsorbed in monolayer quantities on GaAs(110). We have chosen this surface because, in ultrahigh vacuum, the clean and well-ordered (110) surface is the most easily and reproducibly prepared of the low-index faces of GaAs. The (110) surface also exhibits an asymmetry about a principle crystallographic axis, creating a unique local environment at the surface that presents both filled and empty dangling bonds and has been shown to be useful for orienting molecular adsorbates.⁴ Our experimental techniques include time-of-flight studies to examine desorbed-product channels and temperature-programmed desorption for investigation of surface-confined products. Our measurements yield the photoreaction cross sections at different irradiation wavelengths and allow comparison of these same quantities with the corresponding values for gas-phase species.

A further interesting feature of our results is that they illustrate the utility of using photochemistry to form reactive intermediates at surfaces. In our case, we utilize these intermediates to probe both the nature and the extent of the photoinduced reaction of the adsorbed thiols. The use of these intermediates is facilitated by our earlier studies of the thermal chemistry of organosulfur compounds.⁵

2. Experimental Section

The experiments are conducted in an ultra-high-vacuum (UHV) surface analysis system (base pressure $\approx 2 \times 10^{-10}$ Torr), which has been described elsewhere.⁶ The system consists of a multilevel UHV vessel equipped with a low-energy electron diffraction (LEED) system, a quadrupole mass spectrometer (QMS), an effusive-beam gas doser, and a liquid nitrogen (LN_2) cooled crystal manipulator. For temperature-programmed desorption (TPD) experiments, the crystal is heated at a fixed rate (2.5 K/s) by passing a computer-controlled current through the Mo foil to which the crystal is mounted. The QMS is housed

* Corresponding author. Phone: 631 344-4412. E-mail: nicholas@bnl.gov.

[†] Columbia Radiation Laboratory, Columbia University.

[‡] Brookhaven National Laboratory.

[§] Current address: Chemistry Department, Brookhaven National Laboratory, Upton, NY 11973.

^{||} Materials Science Program, Department of Applied Physics and Applied Mathematics, Columbia University.

in a differentially pumped chamber that is joined to the surface analysis chamber by a 3-mm aperture. The doser consists of a ~ 0.01 -mm aperture mounted ~ 10 cm upstream of the end of a stainless steel tube with an inside diameter of 6 mm. This arrangement affords TPD desorbate flux measurements with low background levels.

An excimer laser operating at 193 nm (ArF) or 248 nm (KrF) is used to provide the UV radiation. The photon flux is measured at the chamber laser window by a thermopile detector. Typical exposures are performed at approximately 20 mW/cm^2 at a repetition rate of 20 Hz, i.e., approximately 1 mJ/cm^2 per pulse. The laser pulse duration is ~ 20 ns.

The $1 \times 1 \times 0.1$ cm GaAs crystals [Atramet, (110) orientation, n-type, Si-doped, $1.4 \times 10^{17} \text{ cm}^{-3}$ carrier concentration] are cleaned after their introduction into the UHV system by repeated cycles of Ar^+ sputtering and annealing at 840 K. The surface order of the bare surface is judged by the observation of a sharp, intense, low-background-level LEED pattern at room temperature and low incident electron energies (~ 20 – 30 eV).

The experiments primarily examined the photochemistry of adsorbed methanethiol (CH_3SH); however, limited experiments were also done with methyl disulfide (CH_3SSCH_3). The $\text{CH}_3\text{-SH}$ (Aldrich, 99.5%) was used without further purification, whereas the liquid CH_3SSCH_3 (Aldrich, 99.5%) was purified by removal of more volatile constituents with several freeze–pump–thaw cycles. The overlayers were grown by exposing the LN_2 -cooled crystal to the flux generated by expanding the vapor of the compound of interest through the pinhole doser from a fixed volume at a known initial pressure, typically 5 Torr, for a predetermined period of time. The volume behind the pinhole can be abruptly filled and evacuated, providing a well-defined exposure period. We find that this method affords coverage reproducibility on the order of 2% of a monolayer.

3. Results

3.1. Photoinduced Chemistry of CH_3SH . Methanethiol monolayers were prepared by exposure of the clean, ordered GaAs(110) surface to an effusive flux of methanethiol, followed by annealing to 250 K. Exposure time and annealing temperature were based on the TPD signature for a saturated monolayer, which was determined in our earlier TPD measurements.⁴ This study indicated that methanethiol molecularly adsorbs on the (110) surface and desorbs at a temperature of 310 K,⁵ corresponding to an activation energy of desorption of 0.8 eV.⁵ A TPD spectrum of a full monolayer, measured with the QMS tuned to a mass-to-charge ratio (m/e) of 47 (CH_3S), is given in the uppermost desorption wave of Figure 1.

A one-monolayer-covered surface was then irradiated with $\sim 1 \text{ mJ/cm}^2$ of pulsed UV radiation at 193 nm. A sequence of TPD spectra, recorded after exposure to a series of successively increasing number of UV pulses, is also shown in Figure 1. These measurements show that UV irradiation results in a clear and progressive decrease in the intensity of the $m/e = 47$ desorption wave peaked at 310 K. This decrease must be due to a photoinduced reaction that results in a decrease in the amount of adsorbed molecular methanethiol.

The surface photochemistry was first examined by identification of the photofragments ejected during irradiation using the time-of-flight (TOF) capability of the QMS. Measurements made with the QMS tuned to m/e ratios of 15 (CH_3), 47 (CH_3S), and 48 (CH_3SH) indicated that relatively small quantities of photofragments are ejected. Because the largest signals were observed for ejected fragments of m/e 47, we concluded that

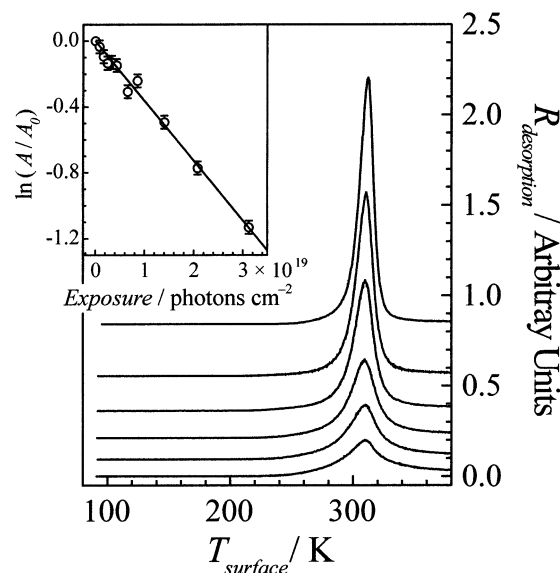


Figure 1. Sequence of TPD spectra recorded after irradiation of a CH_3SH monolayer adsorbed on GaAs(110). The detected fragment is CH_3S^+ . The top spectrum is obtained without irradiation by pulses of 193-nm light. The sequence of traces from top to bottom shows progressively greater UV exposure. A plot of the natural logarithm of the relative integrated intensity of the desorption wave versus UV exposure, in terms of photons per square centimeter, is given in the inset. The spectra have been shifted vertically for clarity.

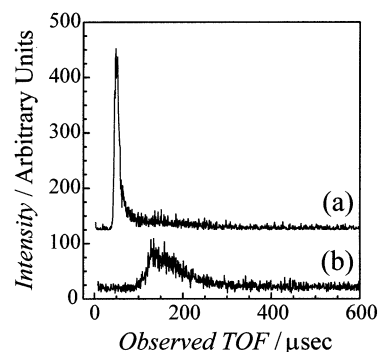


Figure 2. Comparison of TOF spectra recorded during irradiation of monolayers of (a) CH_3Br and (b) CH_3SH at 193 nm, $\sim 1.3 \text{ mJ/pulse}$. The spectrum for CH_3Br shows methyl radical desorption at a kinetic energy (~ 1.4 eV) consistent with dissociation via electron attachment and represents the accumulation of data over 400 pulses. The spectrum for CH_3SH shows CH_3S desorption accumulated over 3×10^4 pulses. The CH_3Br spectrum has been shifted vertically for clarity, and both spectra are uncorrected for velocity-dependent sensitivity factors and ion residence times in the QMS.

the irradiation produced predominantly methyl sulfide (CH_3S) fragments. The weak signals at m/e 15 and 48 were assigned to cracking and reaction with hydrogen in the QMS ionizer, respectively. The angular distribution was broad and featureless and peaked at the surface normal. A search for other ejected photofragments, particularly those corresponding to the methyl radical, i.e., detected by CH_3^+ , as well as variation of the angle of detection yielded no evidence of ejection of other products, nor evidence of any off-normal-oriented angular lobes of photofragments.

A typical TOF measurement of CH_3S ejected along the surface normal during 193 nm irradiation is shown in Figure 2b. For comparison we show, in Figure 2a, the TOF spectrum recorded for CH_3 radicals ejected at 45° from the surface normal during irradiation of a methyl bromide monolayer at the same pulse energy. Because the UV photochemistry of CH_3Br has

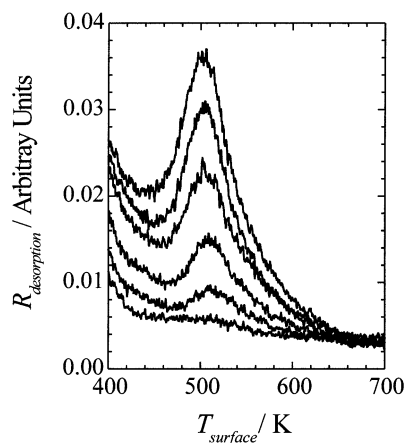


Figure 3. Sequence of TPD spectra recorded at $m/e = 47$ (CH_3S^+) showing an increase in CH_3SCH_3 desorption at ~ 500 K with increased exposure to 193-nm light. Spectra (from top to bottom) correspond to spectra (from bottom to top) in Figure 1 and are shown here without any artificial vertical shift.

been well characterized at a variety of wavelengths and angles,⁶ this comparison provides a relative measure of the ejected photofragment yield. In particular, we note that, even though the methanethiol monolayer received 75 times the photon exposure than did the CH_3Br monolayer, the integrated intensity of the CH_3S fragments is only of the same magnitude as that for the CH_3 from CH_3Br . Further, the spectra are uncorrected for QMS sensitivity factors including fragment velocity and ionization cross section, both of which favor the detection of CH_3S .

The ejection of only CH_3S and the comparatively small amount of products detected, despite the magnitude of the cross section derived from the loss of molecular CH_3SH at the surface (see below), suggest that the main photofragmentation event involves cleavage of the S–H bond and that the resulting CH_3S fragments remain predominantly trapped at the surface. Thus, we expect to find evidence for desorption of one or possibly more species other than methanethiol in postirradiation TPD measurements. In fact, evidence for a reaction product containing CH_3S was found in the high-temperature portion of the desorption spectra recorded for $m/e = 47$. These data are shown in Figure 3. Our measurements show that, as the molecularly adsorbed methanethiol TPD wave progressively decreases with increasing photon exposure (Figure 1), a new feature, peaked at ~ 500 K, begins to develop and increase in intensity (Figure 3).

To investigate the nature of these thermally desorbed surface-bound fragments, TPD measurements were made with the QMS set to detect desorption of various species after irradiation of the surface. These measurements showed that the ~ 500 K desorption wave at $m/e = 47$ (as shown in Figure 3) is actually due to cracking of dimethyl sulfide, molecular weight 62, in the QMS, and that methanethiol and dimethyl sulfide were the predominant molecular species that desorbed after irradiation. The desorption of dimethyl sulfide at ~ 500 K was observed in our prior work on organosulfur molecule thermal chemistry⁵ to be due to the desorption of CH_3SCH_3 , produced by extraction of a sulfur atom from dissociatively adsorbed CH_3SSCH_3 . Therefore, to gain insight into the photoinduced chemistry of methanethiol, we can compare the results for the *thermal* chemistry of methanethiol and the *thermal* chemistry of methyl disulfide with the *photoinduced* chemistry of methanethiol on GaAs(110). Specifically, the results of three TPD measurements in Figure 4, recorded with the QMS tuned to $m/e = 62$,

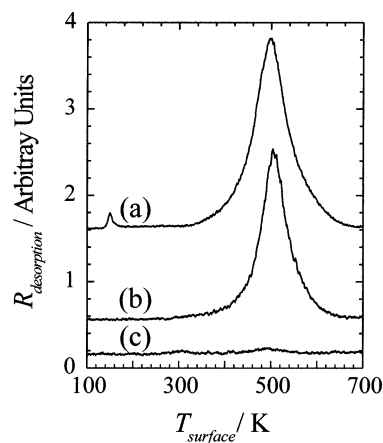


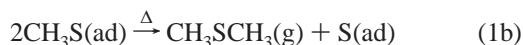
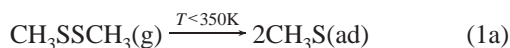
Figure 4. TPD spectra recorded at $m/e = 62$ ($\text{CH}_3\text{SCH}_3^+$) for (a) an unirradiated monolayer of CH_3SSCH_3 , (b) a monolayer of CH_3SH that has been irradiated at 193 nm, and (c) an unirradiated monolayer of CH_3SH .

demonstrate two important points. First, a strong similarity in the chemistries of the photoreacted methanethiol and the thermally reacted methyl disulfide is evident in a comparison of trace a with trace b. Trace a was recorded after deposition of slightly more than 1 ML of CH_3SSCH_3 and shows desorption of CH_3SCH_3 , the product of a purely thermal reaction, reproducing our previously reported work.⁵ Trace b was taken after irradiation of a CH_3SH monolayer and shows the desorption of CH_3SCH_3 with desorption kinetics that are strikingly similar to that in trace a. The significance of this first point is that it provides support for our conclusion that the surface-bound photoproduct is CH_3S (see below).

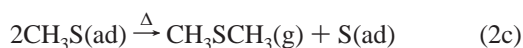
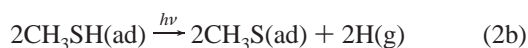
A second important point illustrated by the data in Figure 4 is the unambiguous demonstration that production of CH_3SCH_3 from CH_3SH is the result of a photodissociation reaction and not a thermal reaction. This is readily evident from comparison of traces b and c of Figure 4, which show TPD measurements made for irradiated and unirradiated CH_3SH monolayers, respectively. Clearly, surface irradiation is responsible for the observed chemical transformation in the adsorbed thiol; after irradiation, dimethyl sulfide is desorbed, whereas virtually no dimethyl sulfide is observed to desorb in the absence of radiation. Thus, traces b and c indicate that this chemical transformation cannot be achieved on GaAs(110) by thermal activation alone. We should be careful to note here that, in our previous study of the thermal chemistry of methanethiol on GaAs(110), small amounts of CH_3SCH_3 product were observed.⁵ This can also be seen in trace c of Figure 4. In our previous work, we noted that this was a very minor reaction channel involving only a few mole percent and could be due to either thermal reaction at surface defect sites or formation of methyl disulfide in the gas manifold prior to dosing. Subsequently, we have observed a direct correlation between the time that the methanethiol remained stagnant in the manifold prior to dosing and the amount of CH_3SCH_3 generated thermally at the GaAs-(110) surface (data not shown). This clearly established the action of impurity methyl disulfide molecules in the thermal production of dimethyl sulfide on GaAs(110), although we cannot rule out the possibility that some small percentage of CH_3SCH_3 might be produced thermally from methanethiol at surface defects.

Comparison of the spectra in Figure 4 provides support for our conclusion that the surface-bound photoproduct is CH_3S . Here, we draw on observations gained from our earlier investigation of the thermal chemistry of organosulfur com-

pounds on GaAs(110);⁵ in those experiments, no UV irradiation was present. In that study, we presented evidence that, upon adsorption of methyl disulfide, an adsorbed layer of methyl thiolate (monomethyl sulfide) is formed. When thermally ramped, this surface species desorbs via a second-order process to yield methyl disulfide and surface sulfur. These processes are described by the chemical equations



The need for thermal activation for the first step is not established; however, evidence suggests that the reaction proceeds spontaneously at some temperature below ~ 350 K.⁵ Trace a of Figure 4 is a TPD spectrum corresponding to the second step. Clearly, the 500 K desorption wave is nearly identical to that obtained during TPD of the reaction products generated by irradiation of the methanethiol monolayer at 193 nm (see Figure 4, trace b). This result suggests that the overall photochemistry and subsequent thermal reaction are described by the equations



Reaction 2a describes molecular adsorption characterized by a fairly strong molecule–surface attraction that might involve a hydrogen-bond-like interaction.⁵ Reaction 2b describes the postulated photoinduced chemistry and the trapping of CH_3S at the surface. The fate of the hydrogen atoms, hypothetically shown as ejected neutrals in the above equation, is not known at this time. Reaction 2c describes the subsequent thermal reaction of the trapped CH_3S species to evolve CH_3SCH_3 at ~ 500 K and the production of surface-bound sulfur species. Evidence of the sulfur product is found in the desorption of a GaS species with an onset of ~ 780 K (data not shown).

It is possible that the above observations could be confused by secondary changes in the primary surface products, also due to the presence of the laser irradiation. To investigate this possibility, we irradiated a layer of methyl thiolate, as formed by adsorption of methyl disulfide at 90 K. Trace a of Figure 5 shows the CH_3SCH_3 TPD desorption spectrum measured after deposition of CH_3SSCH_3 ; trace b shows the same measurement made after exposure of the monolayer to 5×10^3 0.6-mJ pulses at 193 nm. These spectra show that, within experimental uncertainty, the shape and integrated area of the 500 K desorption wave are not affected by UV irradiation. Thus, the data indicate that the surface-bound species, which we assign as CH_3S , have a negligible cross section for photoinduced reaction in comparison to CH_3SH .

The simplest interpretation of the results in this section is that irradiation cleaves the S–H bond, a process that is seen, for example, in the gas-phase photochemistry of methanethiol at certain wavelengths, and that the CH_3S fragment is trapped on the surface. The H product might remain on the surface, or it might be ejected. (The poor performance of our QMS at m/e less than 2 made reliable measurements of hydrogen atoms impossible.) The trapping of CH_3S is consistent with the energy and momentum conservation of the photoreaction process. In

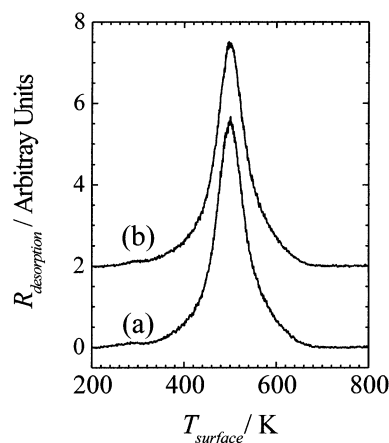


Figure 5. TPD spectra recorded for a monolayer of CH_3SSCH_3 (a) before and (b) after irradiation at 193 nm. The exposure involved 5×10^3 0.6-mJ pulses. The spectra are so similar that, if they are not displaced vertically (as in this figure), they are virtually impossible to distinguish. There is no difference in integrated area under these curves within the experimental error.

particular, a photon energy of 6.4 eV (193 nm) and a S–H bond dissociation energy of 3.93 eV⁷ would leave at most ~ 2.5 eV available for the fragment kinetic energy if no internal excitation occurred in the fragment. For this limiting case, the energy of the fragment can be shown to be equal to $(1 - \beta)E_{\text{avail}}$ where β is the ratio of the masses of the product fragment and the parent molecule. For S–H cleavage with a 6.4 eV photon, $E_{\text{avail}} = 2.5$ eV and $\beta = 0.979$. Thus, the kinetic energy of the CH_3S fragment would be at most 0.05 eV. This value is small compared to the activation energy for desorbing the CH_3S fragment from the GaAs(110) surface and is, thus, consistent with a relatively high probability of surface trapping and lack of ejected photoproducts. Note that these observations do not, in themselves, provide insight into the precise excitation process responsible for bond cleavage.

3.2. Cross Section for Photoassisted S–H Bond Cleavage at 193 nm. The cross section of the photoreaction process can be measured by quantification of the desorbed methanethiol signal as a function of the irradiation time. Rigorously, a cross section for a specific surface photochemical event can be assigned only once the details of the reaction mechanism are determined. Thus, for example, if the process is bond cleavage by direct photolysis, the number of photons incident on an adsorbate molecule is the relevant quantity in determining the cross section, whereas if the process is initiated by photoelectrons, the number of photoelectrons incident on the molecule is the crucial quantity to use in determining the cross-section. In our case, we adopt the common and more empirical approach and simply use the number of incident photons to compute an effective cross section.⁸ Thus, in this convention, the cross section is simply obtained from the slope of the plot of $\ln(N/N_0)$ versus exposure, where N (N_0) is the number of adsorbed CH_3SH molecules after (before) irradiation. The cross section, σ , is obtained from the slope $= -\sigma\gamma$, where γ is the exposure in photons per square centimeter. The calculation uses the integrated area under the TPD wave to quantify the number of unreacted adsorbed molecules remaining on the surface relative to the number of molecules in a full unreacted monolayer.

In the inset of Figure 1 the natural logarithm of N/N_0 is plotted as a function of integrated exposure. Examples of the actual TPD data are also shown in Figure 1. From these data, an effective cross section of 3.6×10^{-20} cm² is obtained for this

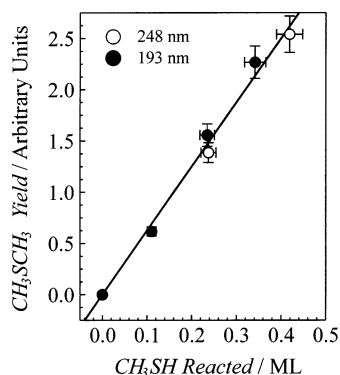


Figure 6. CH₃SH product yield, determined from the increase in area under the $m/e = 62$ TPD wave, as a function of CH₃SH reactant consumption, determined from the decrease in area under the $m/e = 47$ TPD wave. The data show a single linear increase in product yield with reactant consumption.

reaction. This cross section is comparable to that for photoreaction of CH₃Br on the same surface, also using 193 nm, which was obtained in previous measurements.⁶ Note that detailed TOF investigations of CH₃Br photoreactions have shown that in the case of CH₃Br monolayers on GaAs(110), C–Br bond cleavage is due to substrate-photoelectron-mediated reactions. Reactions due to direct photolysis are strongly quenched by resonant electron energy transfer to the substrate.

3.3. Wavelength Dependence. The wavelength dependence of the photoreaction cross section can provide important evidence on the underlying photoreaction mechanisms. An accurate measurement of this quantity can be difficult on surfaces because the optical properties of the surface affect the excitation process. Thus, the absorptivity and reflectivity of GaAs are different at the two wavelengths that we compare here, namely, 248 and 193 nm. Despite this difference, we have measured the effective cross section at these two wavelengths using the procedures described above in section 3.1 for 193-nm irradiation. The results show that the effective cross section is significantly different for the two wavelengths, being a factor of 10 larger at 193 nm.

To further probe the wavelength dependence of the photochemistry, we used TPD to measure the CH₃SCH₃ product yield as a function of the amount of molecular CH₃SH depleted. In this way, we can determine the degree of progress of the photoreaction and relate this quantity directly to the yield of a specific product. In Figure 6, the results of our measurements of the reaction progress are plotted so as to enable a comparison of the chemistry induced by irradiation at 193 and 248 nm. TPD allows for an independent determination of the amount of CH₃SH that is dissociated during irradiation and the amount of CH₃SCH₃ that is produced during the postirradiation thermal reaction. The degree of consumption of the reactant molecules is easily and reliably calibrated, given the integrated signal for the full CH₃SH monolayer. Likewise, the full CH₃SH monolayer provides a reliable calibration of the relative product yield by removing any signal-level variations due to changes in QMS sensitivity. Most important, measuring the relative CH₃SCH₃ product yield as a function of the consumption of the reactant CH₃SH provides a means for probing possible changes in product branching ratios. Specifically, because our comparison of the desorption kinetics for the production of CH₃SCH₃ from the trapped photoproducts indicates that the surface species are the same as for the thermal reaction of CH₃SSCH₃ on GaAs(110), namely, that the trapped intermediate species is CH₃S, any change in the branching ratio for the photoinduced reaction, such as is observed for gas-phase photolysis, leading to the

production of CH₃ would result in a drop in the CH₃SCH₃ yield. Figure 6 demonstrates that, in fact, such a drop is not observed. The measurements show that the product yield is the same in terms of the number of CH₃SCH₃ molecules produced per CH₃SH molecule reacted, indicating that, within experimental uncertainty, the branching ratio for the photoinduced surface reaction does not change with wavelength. If, for example, the probability of cleavage of the C–S bond increased from approximately 0 to ~50% with a change in incident wavelength from 248 to 193 nm (as is observed for gas-phase photolysis), we would expect a corresponding drop in the postirradiation TPD yield of CH₃SCH₃ of ~50%. Figure 6 shows that this is clearly not what is observed.

Thus, our interpretation of all of our data leads us to two conclusions: (1) that the branching ratio for the photoreaction does not depend on wavelength and (2) that S–H cleavage dominates. The first conclusion is most directly supported by the data described above. The only inherent assumption here is quite reasonable, namely, that two different reaction channels [e.g., CH₃S(ad) + CH₃(ad) → CH₃SCH₃(g) and 2CH₃S(ad) → CH₃SCH₃(g) + S(ad)] cannot form the product with the same reaction kinetics (i.e., the single desorption wave observed at ~500 K). The second conclusion hinges on the assumption that S–H cleavage leads to CH₃SCH₃ product, whereas C–S cleavage does not. At present, we have no direct evidence to prove this assertion, but the indirect evidence is strongly supportive. Our TPD studies of CH₃SSCH₃ on GaAs(110) show dissociative adsorption of a species, which results in thermal generation of CH₃SCH₃ with the same desorption kinetics observed for the CH₃SH photoproducts. The relative reactivity of the S–S linkage due to its partial π character suggests CH₃S as the likely adsorbed species for CH₃SSCH₃ on GaAs(110), as observed on Au(111).⁹ In addition, we have observed minority reaction channels consistent with the desorption of CH₃ and possibly a methyl arsenic species at ~670 K, indicating that adsorbed methyl groups desorb at a significantly higher temperature than that at which CH₃SCH₃ evolution is observed.⁵ Taken together, these facts are consistent with the conclusion that, in both the thermal CH₃SSCH₃ dissociative adsorption and the photoinduced CH₃SH decomposition, the resulting adsorbed species is methanethiolate, leading to our assertion that S–H cleavage dominates the photoinduced chemistry of CH₃SH on GaAs(110).

4. Discussion

4.1. Dissociation Mechanism. To explain the above measurements, we must consider two possible mechanisms for the reaction, that is, direct photolysis and photoinduced dissociative electron attachment. Considering first direct photolysis, Figure 7 shows the cross sections at 248 and 193 nm plotted so as to provide a comparison with the continuous spectrum of the total photoreaction cross section of methanethiol measured in the gas phase by Vaghjiani.¹⁰ Two aspects of this comparison are noteworthy. First the cross section of the adsorbed molecule scales with the gas-phase spectrum: the cross section of the adsorbed methanethiol is nearly 1 order of magnitude less at 248 than at 193 nm, a decrease that closely reproduces the gas-phase behavior. Second, the cross section for dissociation of the adsorbed molecule is 50 times lower than it is in the gas phase. The first result would be consistent with dissociation being the result of direct absorption of a photon by the molecule. As mentioned above, the fact that the cross section is much smaller than that for the gas phase would not be unexpected because of the commonly observed strong quenching of

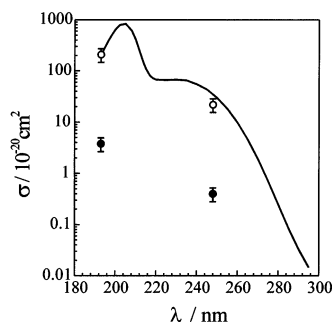


Figure 7. Comparison of the gas-phase UV absorption cross section (solid line from ref 10) with the cross section estimated from the measurements described in this work at 193 and 248 nm (filled circles) for CH_3SH adsorbed on GaAs(110). The measured cross sections for the adsorbed species are also shown scaled to the gas-phase value at 193 nm for the purpose of comparing the relative values at the two wavelengths (open circles).

photoexcited adsorbate molecules by energy transfer to a semiconducting or metal substrate.

However, our measurements of the photochemistry of the absorbed molecule are not consistent with earlier measurements of the photodissociation of gas-phase CH_3S , which showed that the S–H/C–S bond cleavage branching ratio is wavelength-dependent. The gas-phase UV absorption spectrum of CH_3SH comprises two broad bands, a lower band centered near 230 nm and an upper band at approximately 205 nm.^{10,11} Photolysis in the longer-wavelength regime involves direct excitation to a state that is repulsive along the S–H coordinate. In contrast, photolysis at shorter wavelengths, ≤ 222 nm, involves excitation to an excited singlet state that is believed to be bound in both the C–S and S–H reaction coordinates. In fact, the *ab initio* potential energy surfaces for this excited state along the S–H and C–S bond coordinates closely resemble those of the ground state, although they are shifted higher in energy by ~ 6.5 eV.¹¹ Dissociation from this higher-lying excited state, then, occurs via internal conversion to the lower excited state. C–S bond scission occurs only as a result of stretching of the C–S bond in the upper state followed by coupling of the upper state to the lower state, and not by direct excitation to the lower state. C–S scission is not seen after direct excitation to the lower state, because the lower state is actually (weakly) bound in the Franck–Condon region along the C–S coordinate. The interplay between these states results in yield ratios that are counterintuitive from a thermodynamic point of view. At lower photon energies, the *stronger* S–H bond is cleaved predominantly. Only with *increasing* photon energy does cleavage of the *weaker* C–S bond become significant. Specifically, for irradiation at wavelengths of ≥ 220 nm, the dissociation event results dominantly in monomethyl sulfide; that is, S–H bond cleavage accounts for $\sim 100\%$ of the products. However, as the wavelength of the exciting radiation is decreased, the importance of C–S bond cleavage dramatically increases such that at 193 nm C–S bond cleavage accounts for 40–50% of the products. In contrast, our measurements of the dissociation of the adsorbed molecule show no indication of any change in the branching ratio as the wavelength is decreased from 248 to 193 nm. This conclusion is drawn from the fact that the CH_3SCH_3 yield per dissociated CH_3SH molecule does not depend on wavelength, as illustrated in Figure 6. As described above, these results are consistent with the operation of a single dissociative channel, namely, cleavage of the S–H bond.

One possible explanation for the adsorption-induced change in the wavelength dependence of the branching ratios could be

a shift in the absorption spectrum. However, usually such shifts are to the red, and thus, the ratio should be shifted in favor of the C–S bond cleavage channel on the substrate. We would not expect the shift to be large enough to open up the C–S channel at 248 nm (5.0 eV); however, we might expect the C–S channel at 193 nm (6.4 eV) to proceed with greater efficiency than in the gas phase. Instead, the yield of CH_3S is identical at both wavelengths.

The failure of a direct photolysis mechanism to provide a simple explanation for our observations leads us to consider a dissociative electron attachment (DEA) mechanism,⁸ wherein “hot” electrons might be captured by adsorbates into an adsorbate affinity level to cause dissociation with relatively high efficiency. Certainly, our measured effective cross section for cleavage of the S–H bond is comparable to that seen for DEA by photoexcited surface electrons for other well-studied surface adsorbate species, e.g., alkyl halides, also on GaAs(110).⁶ In this case, photoabsorption by GaAs at 248 and 193 nm has been shown to generate a distribution of hot electrons. In the case of CH_3Br , the affinity level is located at 2.1–2.4 eV.¹² The similarity of this value with that expected for CH_3SH (see following paragraphs) makes a plausible case that dissociation for the latter occurs via the same mechanism as for CH_3Br .

We are not aware of any gas-phase study of electron attachment to CH_3SH . As regards S–H cleavage, we can look to the work of Sanche and Schulz¹³ and Modelli and co-workers,¹⁴ who used transmission electron spectroscopy to study electron interactions with H_2S and thiophenol, respectively. They identified shape resonances centered at 2.3 and 2.2 eV for H_2S and thiophenol, respectively, that were assigned to electron capture into a $\sigma^*_{\text{S–H}}$ orbital. In the case of H_2S , electron capture by the affinity level results in dissociation (S–H cleavage) with a peak cross section of $\sim 10^{-18}$ cm².¹⁵ It is reasonable to predict a similarly relatively low-lying affinity level for CH_3SH . Regarding C–S cleavage, we find that electron transmission spectroscopy shows σ^* shape resonances involving S–C antibonding orbitals for $(\text{CH}_3)_2\text{S}_x$ with $x = 1, 2$, and 3, molecules closely related to CH_3SH .¹⁶ The trend in the location of the $\sigma^*_{\text{S–C}}$ resonance is to higher energy with decreasing sulfur content, suggesting that the $\sigma^*_{\text{S–C}}$ resonance for CH_3SH should be located at ~ 3.25 eV [the $\sigma^*_{\text{S–C}}$ location for $(\text{CH}_3)_2\text{S}$]. We have not found gas-phase measurements correlating capture into this orbital with S–C bond scission. Nevertheless, the data for these closely related molecules indicate that relatively low-lying affinity levels with antibonding character exist for CH_3SH and argue for the likelihood that photoinduced dissociation of the adsorbed molecule is the result of dissociative electron attachment.

Finally, with regard to the observed branching ratio, the persistence of preferential cleavage of the S–H bond at shorter wavelengths might simply reflect the fact that an electron-based mechanism yields a different branching ratio than simple photon-induced bond cleavage. Thus, the photoinduced cleavage of our adsorbed molecule might simply be due to preferential capture of an electron into the relatively low-lying $\sigma^*_{\text{S–H}}$ affinity level. In this scenario, the preference for S–H cleavage over S–C cleavage would be expected for at least two reasons. First, as explained above, the $\sigma^*_{\text{S–H}}$ affinity level is expected to occur at a lower energy than the $\sigma^*_{\text{S–C}}$ affinity level, making it more accessible to the relatively low-energy hot electrons generated by photon absorption in the GaAs. Second, the general trend for an increase in anion lifetime with decreasing vertical attachment energy¹⁷ would also favor the dissociation via capture into the $\sigma^*_{\text{S–H}}$, as opposed to the $\sigma^*_{\text{S–C}}$, affinity level.

In summary, the observations and measurements presented here unfortunately do not provide an unambiguous identification of the reaction mechanism. However, as pointed out above, in many previous experiments, it has been found that direct photoreaction reactions are heavily quenched on GaAs and Si, whereas electron-transfer reactions are less so. This important observation, in connection with the above lines of argumentation, causes us to favor a reaction initiated by photoelectrons.

4.2. Comparison to the Chemistry of Methanethiol on Other Surfaces. Because of the possible role of thiols as intermediates in hydrosulfurization,¹⁹ as well as the problem of sulfur poisoning of catalysts by sulfur-containing organics in fuels,²⁰ the chemistry of organosulfur compounds on the surfaces of metals, oxides, carbides, and metal/oxide model catalysts has been the subject of detailed investigation. The chemistry of methanethiol has been studied on a number of metals, including Ni(111), Ni(110), Ni(100), Pt(111), Mo(110), W(001), W(211), Cu(100), Fe(100), and Fe(110).²¹ The interaction of atomic sulfur with transition metals is strong (~ 3.5 – 6.1 eV).²⁰ The cleavage of the S–H bond requires little or no thermal activation and proceeds spontaneously at low temperatures, even below 100 K.²² The predominant surface-bound intermediate species is methyl thiolate (monomethyl sulfide), although thioformaldehyde (SCH_2) has also been observed to form.²³ Typically, C–S bond cleavage occurs in the 250–400 K range,^{20,21} although cleavage has been observed to occur at temperatures as low as 100 K in the case on Ni films on W(001).²⁴ Ultimately, cleavage of the S–H and C–S bonds results in the production of dihydrogen and methane (and sometimes ethane²⁵), with reaction to form methane competing with molecular decomposition to form adsorbed C, S, and H. The product branching ratio is dependent on the substrate, the coverage, and the presence of coadsorbates. Very similar statements can be made for the cases of Si(100),²⁶ MoC_x ,²⁷ and defective MoS_2 ²⁸ and TiO_2 ²⁹ surfaces. That cleavage of the C–S bond at relatively low temperature is the rule for these systems stands in stark contrast to our observations on GaAs, both for the thiolate generated thermally from methyl disulfide⁵ and for the thiolate generated by photoactivation of methanethiol, as reported in this paper.

Aside from the case of GaAs(110), there are notable exceptions to the general rule that thiolates decompose to form methane and adsorbed C, S, and H. On Au(111), for example, the Au–S interaction is sufficiently weak that methanethiol is molecularly chemisorbed and desorbs around 220 K. In contrast, methyl disulfide reacts with Au(111) to form thiolates, which, upon heating, associatively desorb as methyl disulfide at around 500 K.³⁰ Thus, whereas Au(111) resembles GaAs(110) in that it strongly but molecularly binds methanethiol, the behaviors of thiolates on the two surfaces are quite distinct. Whereas, on GaAs(110), we observe elimination of a S from two thiolates to form dimethyl sulfide, such a pathway is not observed on Au(111).

Another exception to the above-described trend is “perfect” TiO_2 (110) (i.e., TiO_2 prepared in such a way as to minimize point defects²⁹), upon which no dissociation of methanethiol is observed. Density functional calculations show that the binding of CH_3SH can be attributed to Ti–S interactions involving the occupied lone pairs of the S and the empty dangling bonds of the Ti,²⁹ in a manner very similar to that proposed for GaAs(110), on the basis of chemical intuition and the large desorption activation energy.⁵ On perfect TiO_2 , the lack of electron density due to the presence of the band gap prevents cleavage of the S–H bond. Addition of mid-gap states due to O atom vacancies

provides the requisite electron density for S–H cleavage to proceed. However, the interaction of the thiolate with the O-atom vacancy is so strong that $\text{CH}_3\text{S}-\text{SCH}_3$ bonding is prevented.²⁹ By contrast, our results for GaAs(110) indicate that photons can be used to activate methanethiol and generate thiolates on a surface such that subsequent thermal activation can result in $\text{CH}_3\text{S}-\text{SCH}_3$ interactions, ultimately leading to the formation of CH_3SCH_3 . Thus, by trapping the intermediates on the appropriate surface, new reaction pathways not otherwise observed become possible. One would expect a similar phenomenon to occur with photoexcitation of methanethiol on perfect titania.

In summary, the chemistry of the photogenerated thiolate species on GaAs(110) is unique in the context of previously reported organosulfur–surface chemistries. The S–surface interaction is strong enough to bind the thiolate at high enough temperatures to allow thermally activated “dimerization”, which ultimately results in the elimination of a sulfur atom, observed to desorb as GaS at much higher temperatures. However, the S–surface interaction is not so strong that it prevents dimerization or weakens the C–S bond to the extent that the thiolate decomposes during heating to produce methane at temperatures low enough that dimerization is preempted in favor of decomposition, as occurs on metals or at defects on oxide surfaces.

5. Conclusions

In the present work, we detail measurements of the photo-induced surface chemistry of a model organosulfur compound, methanethiol, with an eye toward exploring the perturbations in its photoresponse that are introduced by adsorption on GaAs(110). We also seek to understand any new chemical pathways made available by trapping the photoreaction products at the surface. We find the photodissociation cross section of the adsorbed molecules to be strongly altered from that of its gas-phase counterpart. The dissociation cross section measured for adsorbed methanethiol at 193 nm is a factor of 50 less than that for the gas phase. We also find that the photodissociation of the adsorbed state of methyl disulfide is even more strongly suppressed, with a cross section more than 1 order of magnitude smaller than that of adsorbed methanethiol and approximately 2 orders of magnitude smaller than that found for gas-phase methyl disulfide. This suppression is consistent with earlier TPD measurements, which indicate that methyl disulfide dissociatively adsorbs on GaAs(110) in the form of a thiolate. It is also consistent with electron-irradiation experiments, which show that the onset of electron-stimulated reactions of adsorbed thiolates occurs at approximately 5 eV,¹⁸ well above the ~ 0.9 eV maximum kinetic energy of electrons photoemitted from GaAs under 193-nm irradiation.

Of particular interest is the observation that surface-bound products of the methanethiol photoreaction react during postirradiation TPD measurements to produce dimethyl sulfide with the same desorption kinetics observed for the thermal reaction of methyl disulfide. This result is consistent with the photoinduced scission of the S–H bond of the adsorbed methanethiol, resulting in the formation of thiolates that are trapped at the surface after photoproduction. These thiolates react with second-order desorption kinetics to produce dimethyl sulfide during postirradiation TPD measurements. Comparison of these results with the abundant literature detailing the thermal chemistry of methanethiol on a variety of surfaces indicates that our results represent an interesting example of a new reaction pathway provided by the surface trapping of photogenerated reaction intermediates that is not observed following simple thermal excitation at a semiconductor, metal, or oxide surface.

Finally, we find that the dimethyl sulfide yield is invariant with respect to change of the excitation wavelength from 193 to 248 nm. This suggests an invariance in the photoinduced product branching ratio, which stands in contrast to a marked wavelength dependence observed for direct photolysis in the gas phase. This result indicates an enhancement in bond specificity of the cleavage process and suggests that the mechanism for photoinduced dissociation on GaAs(110) is photoinduced dissociative electron attachment.

Acknowledgment. We thank José Rodriguez and Abneesh Srivastava for several helpful discussions. We acknowledge support of this work by the DOE under Grant DE-FG02-90ER14104. We also thank the NSF for funding of the instrumentation under Grant DMR 99-03704.

References and Notes

- (1) Schreiber, F. *Prog. Surf. Sci.* **2000**, 65, 151 and references therein.
- (2) Sheen, C. W.; Shi, J.-X.; Mårtensson, J.; Parikh, A. N.; Allara, D. L. *J. Am. Chem. Soc.* **1992**, 114, 1514.
- (3) Bain, C. D. *Adv. Mater.* **1992**, 9, 591.
- (4) Yang, Q. Y.; Schwarz, W. N.; Lasky, P. J.; Hood, S. C.; Loo, N. L.; Osgood, R. M., Jr. *Phys. Rev. Lett.* **1994**, 72, 3068.
- (5) Camillone, N., III; Khan, K. A.; Osgood, R. M., Jr. *Surf. Sci.* **2000**, 453, 83.
- (6) Camillone, N., III; Khan, K. A.; Lasky, P. J.; Wu, L.; Moryl, J. E.; Osgood, R. M., Jr. *J. Chem. Phys.* **1998**, 109, 8045 and references therein.
- (7) McMillen, D. F.; Golden, D. M. *Annu. Rev. Phys. Chem.* **1982**, 33, 493.
- (8) Zhou, X.-L.; White, J. M. *Laser Spectroscopy and Photochemistry on Metal Surfaces*; Dai, H.-L., Ho, W., Eds.; World Scientific: Singapore, 1995; Part II.
- (9) Nuzzo, R. G.; Zegarski, B. R.; Dubois, L. H. *J. Am. Chem. Soc.* **1987**, 109, 733.
- (10) Vaghjiani, G. L. *J. Chem. Phys.* **1993**, 99, 5936.
- (11) Jensen, E.; Keller, J. S.; Waschewsky, G. C. G.; Stevens, J. E.; Graham, R. L.; Freed, K. F.; Butler, L. J. *J. Chem. Phys.* **1993**, 98, 2882.
- (12) Modelli, A.; Scagnolari, F.; Distefano, G.; Jones D.; Guerra, M. *J. Chem. Phys.* **1992**, 96, 2061.
- (13) Sanche, L.; Schulz, G. J. *J. Chem. Phys.* **1973**, 58, 479.
- (14) Modelli, A.; Jones, D.; Colonna, F. P.; Distefano, G. *Chem. Phys.* **1983**, 77, 153.
- (15) Fiquet-Fayard, F.; Ziesel, J. P.; Azria, R.; Tronc, M.; Chiari, J. J. *Chem. Phys.* **1972**, 56, 2540.
- (16) Dezarnaud-Dandine, C.; Bournel, F.; Tronc, M.; Jones, D.; Modelli, A. *J. Phys. B: At. Mol. Opt. Phys.* **1998**, 31, L497.
- (17) Pearl, D. M.; Burrow, P. D. *J. Chem. Phys.* **1994**, 101, 2940.
- (18) Olsen, C.; Rowntree, P. A. *J. Chem. Phys.* **1998**, 108, 3750.
- (19) Rufael, T. S.; Prasad, J.; Fischer, D. A.; Gland, J. L. *Surf. Sci.* **1992**, 278, 41.
- (20) Rodriguez, J. A.; Hrbek, J. *Acc. Chem. Res.* **1999**, 32, 719.
- (21) Friend, C. M.; Chen, D. A. *Polyhedron* **1997**, 16, 3165.
- (22) Batteas, J. D.; Rufael, T. S.; Friend, C. M. *Langmuir* **1999**, 15, 2391.
- (23) Koestner, R. J.; Stöhr, J.; Gland, J. L.; Kollin, E. B.; Sette, F. *Chem. Phys. Lett.* **1985**, 120, 285.
- (24) Mullins, D. R. *J. Phys. Chem B* **1997**, 101, 1014.
- (25) Sexton, B. A.; Nyberg, G. L. *Surf. Sci.* **1986**, 165, 251.
- (26) Zhu, Z.; Srivastava, A.; Osgood, R. M., Jr. Unpublished results.
- (27) Rodriguez, J. A.; Dvorak, J.; Jirsak, T. *J. Phys. Chem. B* **2000**, 104, 11515.
- (28) Wiegenstein, C. G.; Schulz, K. H. *J. Phys. Chem. B* **1999**, 103, 6913.
- (29) Liu, G.; Rodriguez, J. A.; Chang, Z.; Hrbek, J.; González, L. *J. Phys. Chem. B* **2002**, 106, 9883.
- (30) Nuzzo, R. G.; Zegarski, B. R.; Dubois, L. H. *J. Am. Chem. Soc.* **1987**, 109, 733.